36E.0 IN-SITU CHARACTERIZATION OF MICROSTRUCTURAL EVOLUTION DURING SIMULATED ADDITIVE MANUFACTURING IN MODEL ALLOYS

Brian Rodgers (Mines)
Faculty: Amy Clarke (Mines)
Industrial Mentor: Joe McKeown (LLNL), Saryu Fensin (LANL), Edwin Schwalbach (AFRL), Neil Carlson (LANL)

This project initiated in Fall 2019 and aspects are supported by a Multidisciplinary University Research Initiative (MURI) project funded by the Office of Naval Research (ONR), the Office of Science, Basic Energy Sciences (BES) and the National Nuclear Security Administration (NNSA) Laboratory Residency Graduate Fellowship (LRGF). The research performed during this project will serve as the basis for a Ph.D. thesis program for Brian Rodgers.

36E.1 Project Overview and Industrial Relevance

Laser Powder Bed Fusion (L-PBF) Additive Manufacturing (AM) is an attractive technology for manufacturing turbine and aerospace components. However, the processing effects of L-PBF on microstructural evolution are not well understood. This project will develop a fundamental understanding of solidification phenomena under AM conditions in model alloys. Emphasis is placed on *in-situ* experimentation at the Advanced Photon Source (APS) at Argonne National Laboratory (ANL) and Dynamic Transmission Electron Microscopy (DTEM) at Lawrence Livermore National Laboratory (LLNL) with model alloys to understand the role of rapid solidification and processing history on microstructural development. Understanding solidification behavior during L-PBF could allow for enhanced predictive capabilities and microstructural control of components produced by AM.

The alloy systems chosen for this work are the Al-Ag system and two model ternary Ni-base superalloys with different Mo and Al contents but identical equilibrium γ' volume fractions. The Al-Ag system was selected because it demonstrates strong chemical segregation behavior due to the system's shallow solidus and liquidus slopes. The nickel alloys, R2 and R4, are single crystals of high pedigree and known orientation and were chosen for their close resemblance to industrially relevant nickel-based alloys.

36E.2 Previous Work

In-situ experiments at the APS have been performed on alloys in the Al-Ag system and the R2 and R4 alloys. A summary of the alloy compositions and an experimental matrix is provided in tables 36E.1 and 36E.2, respectively. Microstructures of the as-solidified samples were analyzed via scanning electron microscopy (SEM) and transmission electron microscopy (TEM).

36E.3 Recent Progress

36E.3.1 LRGF Residency at LANL

The LRGF program includes at least two residencies at NNSA laboratories. The first of these two residencies was at LANL, and focused on developing modelling skills in molecular dynamics (MD). This was a significant professional development opportunity, as Brian had limited experience with modelling prior to this.

The first steps in the residency were learning how MD itself works. This involved literature review of textbooks and similar documents. MD is a simulation method that operates directly with individual atoms or molecules and can handle systems of up to around ten million particles. Individual electronic states are not handled or even truly considered as in atomistic simulations. Instead, MD uses potentials that describe the energy of a particle as a function of various parameters. The simplest such description computes the energy of a particle based on the distances to other particles within a certain cutoff radius. Regardless of the type of potential employed, a system in MD consists only of particles, and macroscopic properties must be extracted using statistical mechanics. Two of the most desirable properties to compute are pressure and temperature.

Macroscopic temperature is directly related to the average kinetic energy a system of particles, and can be computed with **Equation 36E.1**, where T is the temperature, m_k is the mass of a particle, v_k is the velocity of a particle, D the dimensionality of the system, N the number of atoms, and k is Boltzmann's constant [36E.1]. Pressure is related to the kinetic energy of the system and the forces between atoms, resulting in **Equation 36E.2**, where P_{ij} is the pressure along a given direction, subscripts i and j indicate directions, V is the system volume, N_g is the number of "ghost atoms" created through periodic boundary conditions and/or parallelization, r_{ki} is the position of an atom, and F_{kj} is the force on an atom in a direction.

$$T = \sum \frac{m_k v_k^2}{DNk} \qquad (36E.1)$$

$$P_{ij} = \sum_{k=1}^{N} \frac{m_k v_{ki} v_{kj}}{V} + \sum_{k=1}^{N+N_g} \frac{r_{ki} F_{kj}}{V} \qquad (36E.2)$$

Once an understanding of the fundamentals was developed, work moved on to learning how to work with actual MD simulations. While other software packages are available for MD simulations, the most common choice is large-scale atomic/molecular massively parallel simulator (LAMMPS). LAMMPS is a customizable C++ code optimized to run in parallel. As for running actual simulations, the boundary conditions and ensemble to be used must be specified. LAMMPS allow for three types of boundary conditions: periodic, where the simulation cell loops back around on itself at the edges to create what resembles a four dimensional object, fixed where atoms are deleted if they try to move outside the cell, or shrink-wrapped where the cell boundaries are non-periodic and grow or shrink according to the positions of the outermost atoms. An ensemble is used to specify macroscopic system variables that are to be held constant. The behavior of the simulated system strongly depends on which ensemble is used. An incorrect choice of ensemble will lead to a simulation with limited meaning. The methods used by an ensemble to hold variables constant depends on the variable of interest.

Once an understanding of molecular dynamics modelling and LAMMPS itself was developed, the next step was to begin performing simulations to gain a practical understanding. MD simulations can be broadly divided into the categories of static and dynamic. Static simulations do not assign velocities to the particles, and typically involve evaluating the forces between particles and shifting their positions to find energy minima. Since the particles lack velocity, static simulations represent conditions at absolute zero. In contrast, dynamic simulations allow for particles to truly move rather than shift positions into lower energy configurations. Dynamic simulations are necessary for temperature to exist; as **Equation 36E.1** shows, velocity is required for temperature. The static simulations performed were the cold curve and determining the elastic constants. A cold curve, not to be confused with a cooling curve, is the cohesive energy of a crystal as its lattice parameter is changed. This was found by forcing the system into various non-equilibrium states through pure dilation and computing the energy (**Figure 36E.1**). Elastic constants were calculated by perturbing the lattice along various directions and computing the pressure tensor in the new configuration. Care must be taken to keep the perturbations small when evaluating the elastic constants, as large displacements may destabilize the current lattice structure and cause an unintentional change in crystal structure. This is especially likely for systems with TWIP/TRIP behavior, but can occur with any system if the strains used are too large.

The two properties chosen to evaluate with dynamic simulations were the coefficient of thermal expansion and melting temperature. Choosing the correct ensemble for these simulations was critical in order to obtain meaningful results. The simulations for thermal expansion were done by controlling the number of atoms, the pressure, and the temperature to a target value, known as an NPT ensemble. Note that pressure in this case means the total pressure, not the value of a particular component in the pressure tensor. The first step in the procedure for the actual run is to create a cubic simulation cell 50 0 Kelvin lattice parameters long with periodic boundary conditions. After providing the atoms with a seeded random initial Gaussian velocity distribution corresponding to the target temperature, the system is controlled to a pressure of 1 bar and the target temperature with an NPT ensemble. The system then runs long enough to equilibrate (**Figure 36E.2**), at which point the lattice parameter is determined by dividing the cell length by 50 and averaging over time steps where

the pressure is less than 100 bar *and* the temperature is within 1 K of the target (**Figure 36E.3**). Determining melting point requires a more complicated procedure. The core idea of the method is to perform an enthalpy balance between a liquid and a solid. To do so, a simulation cell containing a solid and liquid in contact with each other is necessary. LAMMPS has no commands to easily generate a liquid from the onset as can be done with solids, nor can a liquid be made by randomly assigning atomic positions. Liquids do not have a uniform radial distribution function as random position assignment assumes, and arbitrarily forcing a random distribution generates absurd local pressures leading to a literal explosion of the simulation cell. Instead, a completely solid simulation cell is created and part of it superheated to melt, then cooled to the target temperature. There are multiple ways to achieve this. In this work, it was achieved by grouping the simulation cell into two halves intended to be the solid and the liquid. The remainder of the procedure is explained via diagram in **Figure 36E.4**. The main takeaway is that the output temperature will drift towards the melting temperature if there is a liquid and solid in coexistence, so guesses overshooting will get colder and guesses undershooting will get hotter.

With an understanding of MD and LAMMPS developed, the final step in the project was to review LAVA and make changes before its publication. LAVA is a Python code that can automatically create and submit LAMMPS scripts. The intent is to couple this code with a machine learning method to develop potentials so that the time consuming verification process can be automated. LAVA calculations verified for accuracy were similar to the simulations performed for edification purposes. The two main focuses were the elastic constant and melting point calculation capabilities. Evaluating the elastic constant calculations involved comparing the calculated properties with the expected properties for the potential across a range of crystal structures and potentials. Some of the calculations for more exotic crystal structures required corrections in LAVA to make correct predictions, and the initial strain increment chosen had to be deceased. Predictions were considerably more inconsistent with the melting point calculations in LAVA. The initial method to check for convergence in LAVA used the output temperature from the previous iteration as the input temperature for the current iteration, and declared convergence if the difference between the input and output temperature was small enough. While convenient for its simpler implementation, there are two scenarios that prevent this algorithm from reliably converging. The first issue is potentials with small changes between the input and output for the melting point test over a range of temperatures. Since the convergence test is based solely on the magnitude of the change, small changes can lead to a premature declaration of convergence. The other issue is the noise intrinsic to the temperature in MD. The magnitude of natural temperature fluctuations is inversely proportional to the number of particles; this effect is unnoticeable macroscopically due to the number of particles involved, but becomes significant for systems with only tens of thousands to millions of particles. This intrinsic, unavoidable noise can cause the algorithm to declare convergence by random chance, despite being close to the melting point. The effect of noise was reduced by averaging the temperature over the last ten readouts instead of only taking the very last, but the algorithm used to test convergence itself requires improvement. Therefore, the algorithm was changed from the relative error method to the bisection method (**Figure 36E.5**). Since this algorithm only references the sign of the temperature change rather than its magnitude, it will not stop prematurely. As for noise, the bisection method will still converge at the same rate regardless of noise in the output temperature. This can cause issues with converging to the incorrect value, but there is not yet a method to reliably converge to the correct temperature when the output temperature is noisy without manual intervention.

36E.4 Plans for Next Reporting Period

Future work will involve electron microscopy and compilation of results with the intent of publishing.

- Write papers relating to dendrite orientation transition (DOT) in Al-Ag and Al-Ge and microstructural refinement in Al-Ag
- Perform any TEM required to complete papers

36E.5 References

[36E.1] D. Frenkel, B. Smit, Understanding Molecular Simulation: From Algorithms to Applications (2002)

36E.6 Figures and Tables

Table 36E.1: Compositions of selected alloys.

	Ni (at%)	Al (at%)	Mo (at%)	Ag (at%)
R2	balance	6.6	1.9	N/A
R4	balance	2.8	22.2	N/A
Al-10Ag	N/A	balance	N/A	10
Al-18Ag	N/A	balance	N/A	18

Table 36E.2: Summary of laser parameters used in experiments at the APS. Pulse duration was 1 ms for all spot melts. Parameters for overlapping melts are shown with a forward slash between the parameters for each.

Alloy	Beam power [W]	Raster speed [m/s]	Notes
R2 [110], R2 [111], R4[100], R4 [110]	253.9	1.6	
	139.4	0.5	
	47.8	0.1	
	82.1/82.1	Spot melt	Edge of second pool intersects middle of first
	82.1/253.9	Spot melt	
R2 [110]	517.1	1.6	
	253.9	1	
R4 [100]	517.1	1.6	
	368.3	1.6	
	253.9	Spot melt	
Al-10Ag & Al-18Ag	282.5/282.5	0.1/0.1	Re-rasters with 100% overlap
	368.3/368.3	2/2	
	282.5	0.1	
	368.3	2	

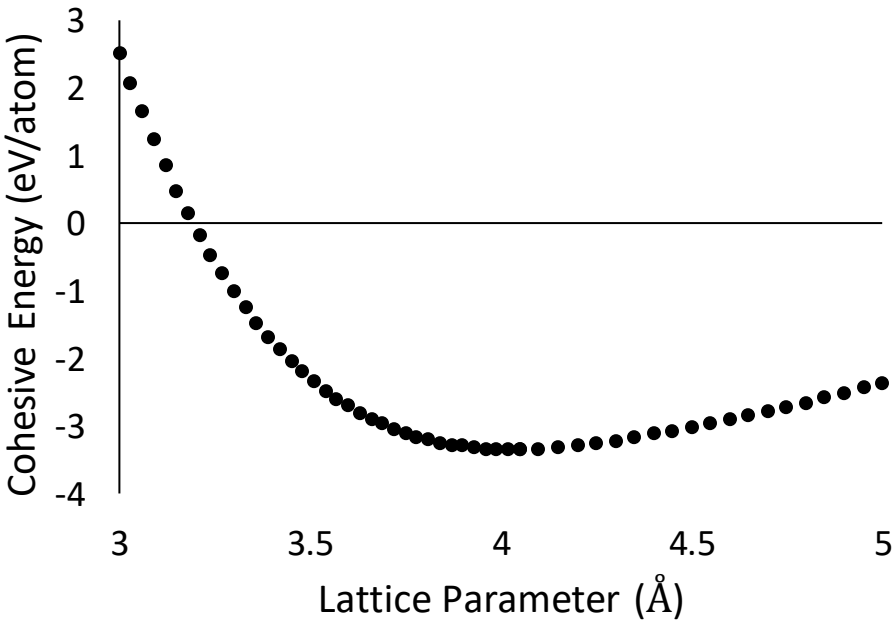

Figure 36E.1: Cold curve for pure Al as computed by changing lattice parameter.

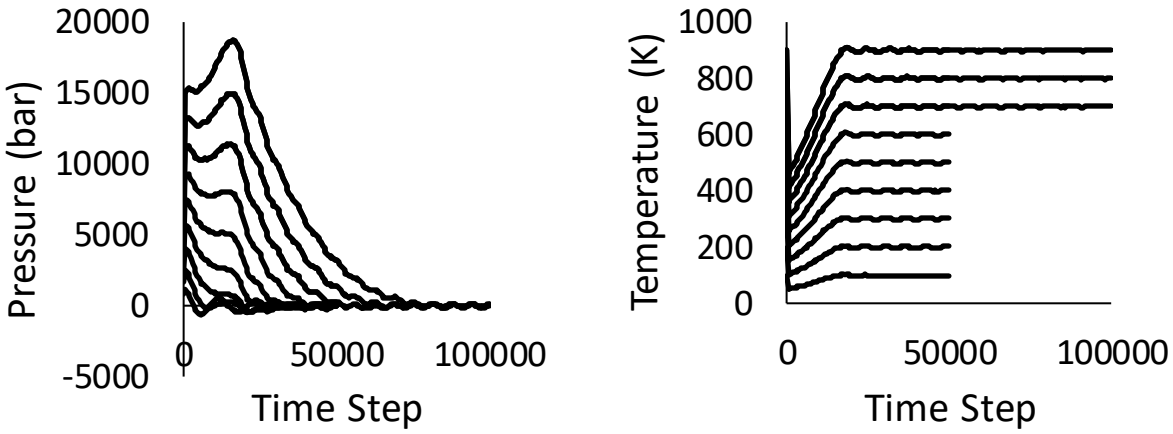

Figure 36E.2: Equilibration of (left) pressure and (right) temperature during determination of CTE for pure Al. The three highest temperature conditions required more time steps to equilibrate, and were run for twice as long to compensate.

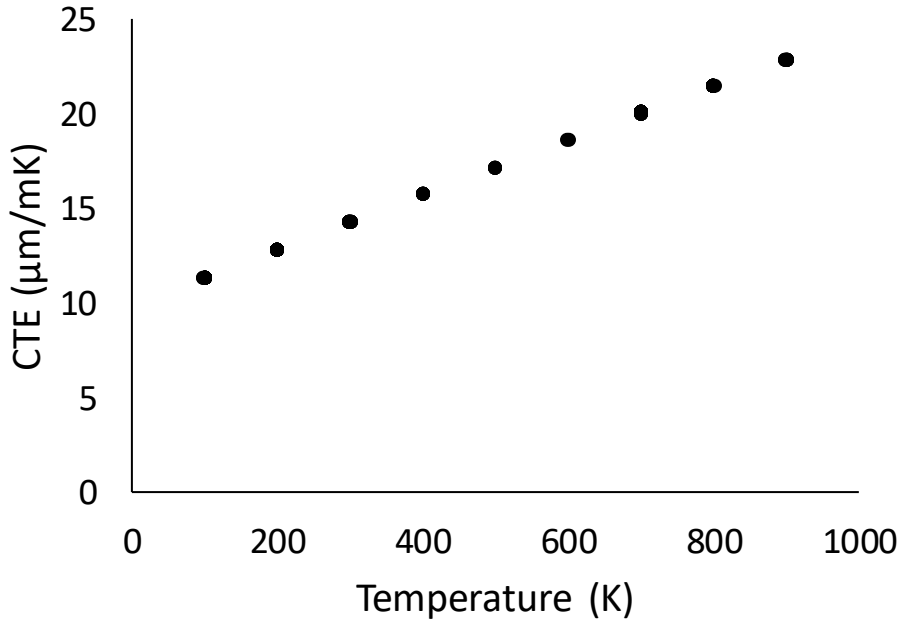

Figure 36E.3: CTE calculated for pure Al up to near the melting point

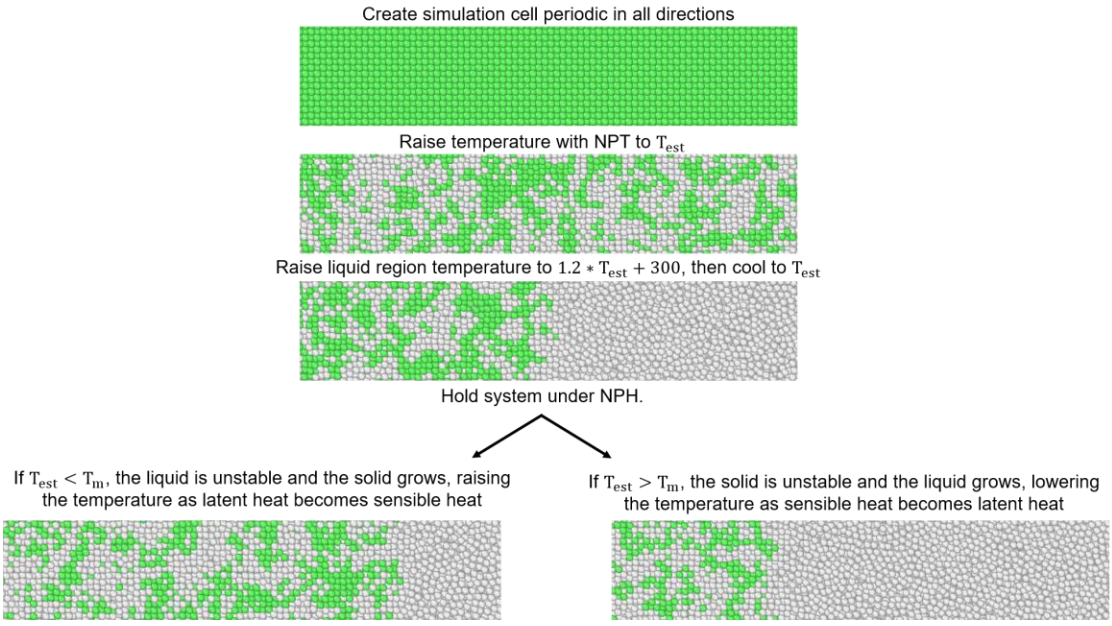

Figure 36E.4: Demonstration depicting how the estimated melting point, T_{est}, can be determined to be greater or less than the actual melting point. Atoms are colorized according to whether they are FCC or not via common neighbor analysis, with crystal regions colored green and non-crystalline regions colored grey. The NPH ensemble refers to holding the system under constant particle count, pressure, and enthalpy.

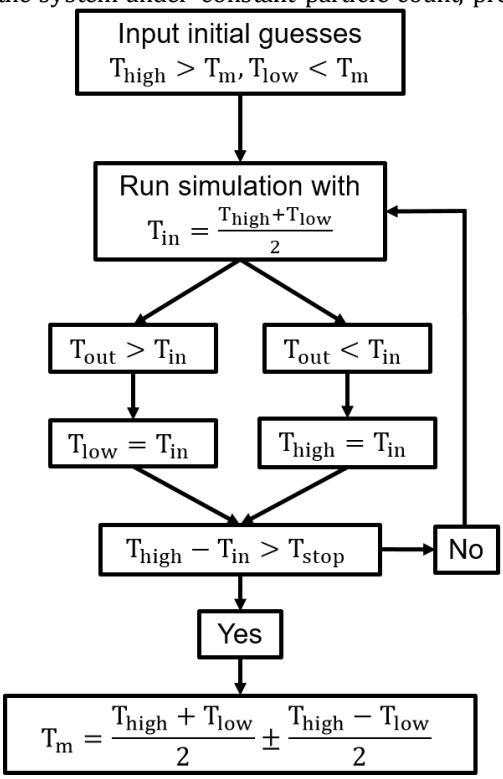

Figure 36E.5: Flowchart showing the implementation of the bisection method in LAVA. T_{high} and T_{low} indicate the upper and lower temperature bounds, respectively. T_m is the melting point and T_{stop} is a user defined criteria. T_{in} and T_{out} are the input and output temperatures for a single simulation run as described in **Figure 36E.4**.